Memorias del 2022 Congreso Nacional de Control Automático
12-14 de Octubre, 2022. Tuxtla Gutiérrez, México.

On the synchronization of selfexcited and hidden attractors

Juan Gonzalo, Barajas-Ramírez *

* *IPICYT, División de Control y Sistemas Dinámicos, Camino a la Presa San José 2055, Col. Lomas 4a CP. 78216, San Luis Potosí, S.L.P., México. (E-mail: jgbarajas@ipicyt.edu.mx).*

Abstract: Many nonlinear systems have complex behaviors where selfexcited and hidden attractors exist and some times coexist. We investigate the synchronization problem for these type systems under two different coupling configurations: *drive-response* and *bidirectional*. In the first scheme, the coupling term in the response subsystem can be design as an output feedback controller to achieve synchronization; while in the latter, since the states of both systems depend on their interaction, the coupling terms are designed in terms of their differences. As observed before synchronized behavior on a hidden attractor is very difficult to achieve. In this sense our results show that for the *drive-response* configuration is relatively simple to impose a synchronized behavior; however, on hidden attractors the region of attraction of the synchronized solution reduces to that of the hidden attractor. Additionally, in a *bidirectional* configuration the region of attraction of the synchronized behavior basically disappears making the design of a static coupling considerably more difficult. We illustrate our results with numerical simulations of systems with hidden and selfexcited attractors.

Keywords: Synchronization, Control of nonlinear systems, hidden attractors, drive-response, bidirectional coupling.

1. INTRODUCTION

Synchronization is a universal and widely studied phenomenon of nonlinear dynamics. In general terms, two or more systems that interact through a subtle coupling are said to be synchronized when their behaviors are correlated in time [Pikovsky *et al.* (2001)]. Depending on the features of their temporal correlation many different types of synchronized behaviors can be defined, including: identical, phase, antiphase and generalized synchronization to mention but a few [Boccaletti *et al.* (2002)]. A particularly important form of the interaction between systems is the so-called *drive-response* configuration [Pecora & Carroll (1990)]. In this case, their one-direction interconnection can easily be interpreted, from the viewpoint of control theory, as a design problem where the coupling term in the response subsystem can be obtained using different control methodologies like robust [Rosas Almeida *et al.* (2006)], adaptive [Hong *et al.* (2001)] and optimal design [Pan & Yin (1997)] techniques. Alternatively to a *drive-response* configuration, two dynamical systems can be *bidirectionally* coupled. In general terms, in this configuration the synchronization problem is more complex since both subsystems depend on each other through their interactions [Boccaletti *et al.* (2002)]. The solutions to bidirectional synchronization problem has been naturally extended to the context of dynamical networks [Boccaletti *et al.* (2006)], where problems like consensus and pinning are significant research topics [Su & Wang (2013)].

In most of the works referred above the systems under consideration are chaotic, that is, their solutions have features like extreme sensitivity to differences in their initial conditions, a dense set of periodic trajectories of all periods, and transitivity between them. These features give rise to well-known strange attractors like Chua's double-scroll and Lorenz's butterfly that can be reached from the vicinity of unstable equilibrium points of the system [Ott (1993)]. This type of attractors are called selfexcited [Leonov & Kuznetsov (2013)]. Recent discoveries about the behavior of dynamical systems far away from their equilibrium points have lead to the classification of attractors as hidden if their basin of attraction do not intersect with a neighborhood of an unstable equilibrium point [Pham *et al.* (2017)].

Hidden attractors are inherently difficult to identify since there is no intersection between their basin of attraction and local unstable manifolds of its equilibrium points. Therefore trajectories starting near an equilibrium point will not lead the hidden attractor. Furthermore, since their basins of attraction and even the attractor itself can be very small and with a fractal geometry, the behavior of coupled systems with hidden attractors can result in amplitude dead [Chaudhuri & Prasad (2014)]. From the general description above, hidden attractors can be found in systems without equilibrium, with an infinite number of equilibria, or with at least one stable equilibrium. Moreover, as shown in [Kuznetsov & Leonov (2014)] hidden and selfexcited attractors can coexist in the same dynamical system. In the literature there is a large set of examples of dynamical systems with hidden attractors. One of the earlier examples comes from the set of simple chaotic flows proposed by Sprott in the 90's [Sprott (1994)], from case A in this reference a plethora of systems without equilibrium points with hidden attractors were proposed in [Wei (2011); Hu *et al.* (2016)]. Other authors have investigated the existence of hidden attractors in dynamical systems with an infinite number of equilibrium points [Jafari & Sprott (2013); Jafari *et al.* (2017)]. Other examples of dynamical systems with hidden attractors have stable equilibrium points are found in [Wang & Chen (2012); Yang & Chen (2008)]. Furthermore, for many systems both types of attractors coexist [Leonov & Kuznetsov (2013); Kuznetsov & Leonov (2014); Dudkowsk (2016); Escalante-González & Campos-Cantón (2020)].

Most of the examples above have nonlinearities with quadratic and higher order terms. However, simpler versions of systems with hidden attractors are derive from piecewise linear (PWL) systems [Leonov & Kuznetsov (2013); Delgado-Aranda *et al.* (2020); Escalante-González & Campos-Cantón (2021)]. A methodology that combines analytical and numerical components can be used to identify hidden attractors in nonlinear dynamical systems using analytical tools, like harmonic linearization and describing function, to establish the existence of stable oscillatory solutions for a linearized version of the original system with a very small nonlinear perturbation. Then, through numerical continuation the perturbation is grown until the perturbed systems is identical to the original system. If this numerical process identifies an oscillation that persists and is not associated with any equilibrium point of the nonlinear system a hidden attractor is found [Dudkowsk (2016)]. Using these ideas selfexcited and hidden attractors can be identify for the same dynamical system [Kuznetsov & Leonov (2014)].

In this contribution, we investigate the synchronization problem of dynamical systems with selfexcited and hidden attractors in both *drive-response* and *bidirectionally* coupled configurations. We propose an output feedback control based design as their interconnections such that identical synchronization is asymptotically achieved. However as observed in [Kuznetsov & Leonov (2014); Chaudhuri & Prasad (2014)] the emergence of synchronized behavior is not easily obtained with the possibility of amplitude dead due to their interactions. We present a justification for the observed difficulty to achieve synchronization on hidden attractors as a consequence of size difference between their basins of attraction that make the synchronization more likely in *drive-response* configurations towards a selfexcited attractor that in all other combinations.

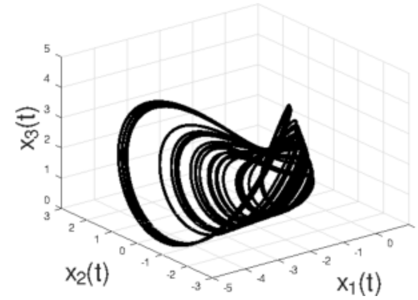

Fig. 1. Hidden attractor of the system without equilibrium points (1) from the initial condition $[-1.6, 0.82, 1.9]^\top$.

The remainder of this contribution is organized as follows. In Section 2 we provide some examples of dynamical systems with hidden attractors of different natures. In Section 3 we describe the synchronization problem for *drive-response* and *bidirectional* configuration along with an output feedback design solution. In Section 4 we use numerical simulations to illustrate our main results. Finally we provide some final remarks and future work.

2. HIDDEN ATTRACTORS OF DYNAMICAL SYSTEMS

By definition an attractor of a dynamical system without equilibrium points is hidden. For example, the following modification of the Sprott system case A [Wei (2011)]:

$$\begin{aligned} \dot{x}_1(t) &= -x_2(t), \\ \dot{x}_2(t) &= x_1(t) + x_3(t), \\ \dot{x}_3(t) &= 2x_2(t)^2 + x_1(t)x_3(t) - 0.35 \end{aligned} \tag{1}$$

results in the hidden attractor shown in Figure 1.

An interpretation of Chua's circuit is as a continuously connected PWL system. Using this interpretation as inspiration many different hidden attractors have been found in PWL systems [Escalante-González & Campos-Cantón (2020)]. On the other hand, the Sprott systems can be interpreted as generated from the Jerk equation with a nonlinear component [Sprott (1994); Zhang & Zeng (2019)]. Therefore, combining these ideas one can find hidden attractors in systems based on the Jerk equation with PWL nonlinearities like the following system:

$$\begin{bmatrix} \dot{x}_1(t) \\ \dot{x}_2(t) \\ \dot{x}_3(t) \end{bmatrix} = \begin{bmatrix} 0 & 1 & 0 \\ 0 & 0 & 1 \\ -0.7 & -0.5 & -1 \end{bmatrix} \begin{bmatrix} x_1(t) \\ x_2(t) \\ x_3(t) \end{bmatrix} + \begin{bmatrix} 0 \\ 0 \\ 1 \end{bmatrix} F(x_1(t)) \tag{2}$$

with $F(x_1(t)) = -\frac{1}{2}(3.5)(|x_1(t)+1| - |x_1(t)-1|)$, which results in the selfexcited attractor and the coexisting hidden attractors in Figure 2.

In the following Section we describe a solution for the synchronization problem in both the *drive-response* and *bidirectional* configuration.

3. THE SYNCHRONIZATION PROBLEM

Consider two coupled identical dynamical systems:

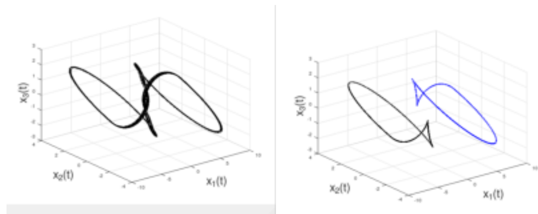

Fig. 2. Coexisting selfexcited and hidden attractors for (2) from the initial conditions $[0.1, 0.1, 0.1]^\top$(self) $[\mp 0.9488, \pm 2.1717, \mp 2.1652]^\top$ (hidden)

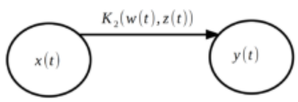

Fig. 3. *Drive-response* scheme

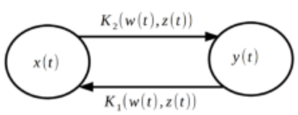

Fig. 4. *Bidirectional* scheme

$$\begin{aligned} \dot{x}(t) &= F(x(t)) + K_1(w(t), z(t)) \\ w(t) &= Cx(t) \end{aligned} \tag{3}$$

$$\begin{aligned} \dot{y}(t) &= F(y(t)) + K_2(w(t), z(t)) \\ z(t) &= Cy(t) \end{aligned} \tag{4}$$

where $x(t), y(t) \in \mathbf{R}^3$ are the state variables; $F(\cdot) : \mathbf{R}^3 \to \mathbf{R}^3$ describes the system's dynamics, which is usually nonlinear and at least locally Lipschitz. The variables $w(t) \in \mathbf{R}$ and $z(t) \in \mathbf{R}$ are the outputs of the corresponding systems with $C \in \mathbf{R}^{1\times 3}$. While the coupling functions $K_i(\cdot,\cdot) : \mathbf{R}^6 \to \mathbf{R}^3$ for $i = 1, 2$ are to be design such that:

$$\lim_{t\to\infty} ||x(t) - y(t)|| = 0 \tag{5}$$

In other words, the coupling functions $K_i(\cdot,\cdot)$ are to be design such that systems (3) and (4) *asymptotically* achieve *identical synchronization*. As shown in Figure **??**, we have two coupling configurations:

- *Drive-Response* configuration (Figure 3) which correspond to the coupled system (3)-(4) with $K_1(\cdot,\cdot) = 0$ and $K_2(\cdot,\cdot) \neq 0$
- *Bidirectional* coupling configuration (Figure 4) for the coupled systems (3) and (4) with $K_1(\cdot,\cdot) \neq 0$ and $K_2(\cdot,\cdot) \neq 0$

Additionally, these coupling functions are assume to be linear combinations of the difference between the system's outputs, *i.e. diffusive* symmetric output coupling:

$$\begin{aligned} K_1(w(t), z(t)) = \kappa_1(w(t) - z(t)) = \kappa_1 C(y(t) - x(t)) \\ K_2(w(t), z(t)) = \kappa_2(z(t) - w(t)) = \kappa_2 C(x(t) - y(t)) \end{aligned} \tag{6}$$

where $\kappa_i \in \mathbf{R}^{3\times 1}$ for $i = 1, 2$ are the coupling gains that are to be design such that (5) is satisfy.

3.1 Synchronization on a drive-response scheme

To verify the emergence of *identical synchronization* in (3)-(4), in the sense of (5), we define the error variables:

$$\begin{aligned} e_1(t) &= x(t) - y(t) \\ e_2(t) &= y(t) - x(t). \end{aligned} \tag{7}$$

with $e_1(t) = -e_2(t)$.

In the *drive-response* configuration, since $K_1(\cdot,\cdot) = 0$, we have the error dynamics:

$$\dot{e}_1(t) = F_1 - \kappa_2 C(y(t) - x(t)) = F_1 - \kappa_2 C e_1(t) \tag{8}$$

where $F_1 = F(x(t)) - F(y(t))$. Then, if the error dynamics (8) are at least locally asymptotically stable the *drive-response* coupled systems (3)-(4) will synchronize.

The stability of (8) can establish using the Lyapunov function

$$V(e_1(t)) = e_1(t)^\top P e_1(t) \tag{9}$$

with $P = P^\top > 0$ a positive definitive matrix. Its derivative along the trajectories of (8) is:

$$\begin{aligned} \dot{V}(e_1(t)) = &F_1^\top P e_1(t) + e_1(t)^\top P F_1 - \\ &e_1(t)^\top[(\kappa_2 C)^\top P + P\kappa_2 C] e_1(t)) \end{aligned} \tag{10}$$

Under the assumption that:

$$P(F(x(t)) - F(y(t))) \leq LP(x(t) - y(t)) \tag{11}$$

with $L \in \mathbf{R}$. The derivative of the Lyapunov function is bounded by

$$\dot{V}(e_1(t)) \leq e_1(t)^\top Q e_1(t) \tag{12}$$

with $Q = 2LP - (\kappa_2 C)^\top P + P\kappa_2 C$. For the error dynamics (8) to be locally asymptotically stable we need to have Q as a negative definitive matrix, that is:

$$2LP - (\kappa_2 C)^\top P + P\kappa_2 C < -\tau I_3 \tag{13}$$

with $\tau > 0$ and I_3 the square identity matrix of dimension three. Then, by choosing κ_2 such that (13) is satisfied the *drive-response* coupled system (3)-(4) will synchronize.

Example 1. Synchronization of Rössler systems in drive-response configuration

Consider a Rössler system as the drive with $x_2(t)$ as the output:

$$\begin{aligned} \begin{bmatrix} \dot{x}_1(t) \\ \dot{x}_2(t) \\ \dot{x}_3(t) \end{bmatrix} &= \begin{bmatrix} -x_2(t) - x_3(t) \\ x_1(t) + 0.2x_2(t) \\ 0.2 + x_1(t)x_3(t) - 5.7x_3(t) \end{bmatrix} \\ w(t) &= x_2(t) \end{aligned} \tag{14}$$

and the response system coupled at the second variable:

$$\begin{aligned} \begin{bmatrix} \dot{y}_1(t) \\ \dot{y}_2(t) \\ \dot{y}_3(t) \end{bmatrix} &= \begin{bmatrix} -y_2(t) - y_3(t) \\ y_1(t) + 0.2y_2(t) - \kappa_{22}(y_2(t) - x_2(t)) \\ 0.2 + y_1(t)y_3(t) - 5.7y_3(t) \end{bmatrix} \\ z(t) &= y_2(t) \end{aligned} \tag{15}$$

The resulting error dynamics are locally asymptotically stable with $\kappa_2 = [0, 0.5, 0]^\top$. For the numerical simulations in Figure 5 the coupling gain κ_{22} is changed from zero to 0.5 after 150 time units.

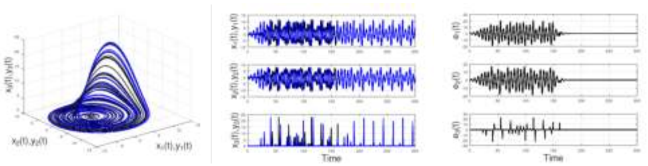

Fig. 5. Synchronization of coupled Rössler systems in *drive-response* configuration with $\kappa_2 = 0.5$ for $t > 150$

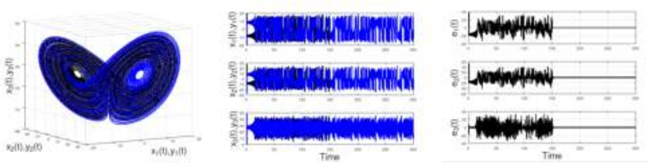

Fig. 6. Synchronization of bidirectionally coupled Lorenz systems $\kappa_{11} = 50$ for $t > 150$

3.2 Synchronization on a bidirectionally coupled scheme

In the *bidirectionally* coupled configuration the error dynamics are:

$$\begin{aligned} \dot{e}_1(t) &= F_1 + \kappa_1 C e_2(t) - \kappa_2 C e_1(t) \\ \dot{e}_2(t) &= F_2 + \kappa_2 C e_1(t) - \kappa_1 C e_2(t) \end{aligned} \tag{16}$$

with $F_2 = F(y(t)) - F(x(t))$. For simplicity, let $\kappa_1 = \kappa_2 = \kappa \in \mathbf{R}^3$, then when synchronization is achieve we have a solution for the coupled systems where:

$$x(t) = y(t) = s(t) \tag{17}$$

That is, when the systems are synchronized the coupling functions in (6) are zero and each node moves as:

$$\dot{s}(t) = F(s(t)) \tag{18}$$

We define a set of error variables to describe the deviation from the synchronized solution as:

$$\begin{aligned} \epsilon_1(t) &= x(t) - s(t) \\ \epsilon_2(t) &= y(t) - s(t). \end{aligned} \tag{19}$$

Then, the deviation error dynamics are:

$$\begin{aligned} \dot{\epsilon}_1(t) &= F_{1s} + \kappa C \epsilon_2(t) - \kappa C \epsilon_1(t) \\ \dot{\epsilon}_2(t) &= F_{2s} + \kappa C \epsilon_1(t) - \kappa C \epsilon_2(t) \end{aligned} \tag{20}$$

where $F_{1s} = F(x(t)) - F(s(t))$ and $F_{2s} = F(y(t)) - F(s(t))$. That in vector form become:

$$\dot{E}(t) = \mathbf{F} + (A \otimes \kappa C)E(t) \tag{21}$$

where $E(t) = \begin{bmatrix} \epsilon_1(t) \\ \epsilon_2(t) \end{bmatrix} \in \mathbf{R}^6$, $\mathbf{F} = \begin{bmatrix} F_{1s} \\ F_{2s} \end{bmatrix} : \mathbf{R}^6 \to \mathbf{R}^6$, $A = \begin{bmatrix} -1 & 1 \\ 1 & -1 \end{bmatrix}$ is the Laplacian matrix of the *bidirectional* connection, and $\otimes$ represents the Kronecker product.

Bidirectional synchronization of the coupled systems (3)-(4) is achieved if the deviation error dynamics (21) are at least locally asymptotically stable around its zero solution.

The stability of the deviation error is investigated linearizing (21) at the zero solution, which results in:

$$\dot{E}(t) = [D\mathbf{F}(s(t)) + (A \otimes \kappa C)]\, E(t) \tag{22}$$

where $D\mathbf{F}(s(t)) = [DF(s(t)), DF(s(t))]^\top$ with $DF(\cdot)$ the Jacobian matrix of the system's dynamics. Since A is a Laplacian matrix there is a change of coordinates $E(t) = \Phi[\nu_1(t), \nu_2(t)]^\top$ with Φ constructed with eigenvectors of A, such that the linearized deviation error can be written as:

$$\begin{aligned} \dot{\nu}_1(t) &= [DF(s(t)) + \lambda_1 \kappa C]\, \nu_1(t) \\ \dot{\nu}_2(t) &= [DF(s(t)) + \lambda_2 \kappa C]\, \nu_2(t) \end{aligned} \tag{23}$$

with $\lambda_1 = 0$ and $\lambda_2 = -2$ the eigenvalues of A. Since λ_1 corresponds to the synchronized solution $x(t) = y(t)$ is sufficient to prove that $\dot{\nu}_2(t) = [DF(s(t)) + \lambda_2 \kappa C]\, \nu_2(t)$ is asymptotically stable. Which can be done using the Lyapunov function

$$V(\nu_2(t)) = \nu_2(t)^\top \Pi \nu_2(t) \tag{24}$$

with $\Pi = \Pi^\top > 0$ a positive definitive matrix of appropriate dimension. The derivative along the second equation of (23) is:

$$\begin{aligned} \dot{V}(\nu_2(t)) = \nu_2(t)^\top ([DF(s(t)) + \lambda_2 \kappa C]^\top \Pi \\ + \Pi\, [DF(s(t)) + \lambda_2 \kappa C])\nu_2(t) \end{aligned} \tag{25}$$

The derivative of the Lyapunov function is strictly negative if

$$[DF(s(t)) + \lambda_2 \kappa C]^\top \Pi + \Pi\, [DF(s(t)) + \lambda_2 \kappa C] \leq -\tau_2 I_3 \tag{26}$$

with $\tau_2 > 0$. Then choosing κ such that (26) is satisfied, the coupled system (3)-(4) will bidirectionally synchronize.

Example 2. Synchronization of Lorenz systems in bidirectional coupling configuration

Consider two Lorenz system coupled through their first coordinate:

$$\begin{aligned} \begin{bmatrix} \dot{x}_1(t) \\ \dot{x}_2(t) \\ \dot{x}_3(t) \end{bmatrix} &= \begin{bmatrix} 10(x_2(t) - x_1(t)) - \kappa_{11}(y_1(t) - x_1(t)) \\ 28x_1(t) - x_2(t) - x_1(t)x_3(t) \\ x_1(t)x_2(t) - \frac{8}{3}x_3(t) \end{bmatrix} \\ w(t) &= x_1(t) \end{aligned} \tag{27}$$

and the response system coupled at the second variable:

$$\begin{aligned} \begin{bmatrix} \dot{y}_1(t) \\ \dot{y}_2(t) \\ \dot{y}_3(t) \end{bmatrix} &= \begin{bmatrix} 10(y_2(t) - y_1(t)) - \kappa_{11}(x_1(t) - y_1(t)) \\ 28y_1(t) - y_2(t) - y_1(t)y_3(t) \\ y_1(t)y_2(t) - \frac{8}{3}y_3(t) \end{bmatrix} \\ z(t) &= y_1(t) \end{aligned} \tag{28}$$

The resulting deviation error dynamics are locally asymptotically stable with $\kappa = [50, 0, 0]^\top$. For the numerical simulations in Figure 7 the coupling gain κ_{11} is changed from zero to 50 after 150 time units.

In the following Section we investigate the effectiveness of our solutions to the synchronization problem for systems with hidden attractors.

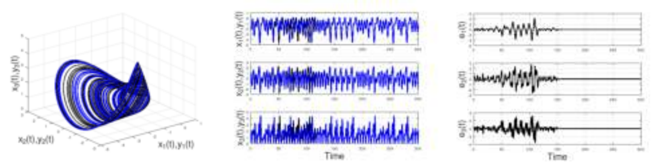

Fig. 7. Synchronization of *drive-response* coupled systems with hidden attractors (1) with $\kappa_3 = 5$ for $t > 150$

4. SYNCHRONIZING TO A HIDDEN ATTRACTOR

We start by considering two identical system with hidden attractors (1) in a *drive-response* configuration

Example 3. For two system without equilibrium points (1) in a *drive-response* configuration

Let the sum of $x_1(t)$ and $x_2(t)$ be the driving signal and the response system be coupled at the third coordinate, then we have:

$$\begin{aligned} \begin{bmatrix} \dot{y}_1(t) \\ \dot{y}_2(t) \\ \dot{y}_3(t) \end{bmatrix} &= \begin{bmatrix} -y_2(t) \\ y_1(t) + y_3(t) \\ 2y_2(t)^2 + y_1(t)y_3(t) - 0.35 \\ -\kappa_{33}[(y_2(t) - x_2(t)) + (y_3(t) - x_3(t))] \end{bmatrix} \\ z(t) &= y_2(t) + y_3(t) \end{aligned} \tag{29}$$

The error dynamics are locally asymptotically stable for $\kappa = [0, 0, 5]^\top$. In Figure 7 the coupling gain κ_{33} is changed from zero to 5.0 after 150 time units.

Next we consider bidirectionally coupled systems with both selfexcited and hidden attractors.

Example 4. Consider two PWL systems (2) with initial conditions such that both have as their solution hidden attractors, then they are *bidirectional* coupled at their third coordinate through their second variable, that is the systems become:

$$\begin{aligned} \begin{bmatrix} \dot{x}_1(t) \\ \dot{x}_2(t) \\ \dot{x}_3(t) \end{bmatrix} &= \begin{bmatrix} x_2(t) \\ x_3(t) \\ -0.7x_1(t) - 0.5x_2(t) - x_3(t) \\ +F(x_1(t)) - \kappa_{32}(y_2(t) - x_2(t)) \end{bmatrix} \\ w(t) &= x_2(t) \end{aligned} \tag{30}$$

and the response system coupled at the third variable:

$$\begin{aligned} \begin{bmatrix} \dot{y}_1(t) \\ \dot{y}_2(t) \\ \dot{y}_3(t) \end{bmatrix} &= \begin{bmatrix} y_2(t) \\ y_3(t) \\ -0.7y_1(t) - 0.5y_2(t) - y_3(t) \\ +F(y_1(t)) - \kappa_{32}(x_2(t) - y_2(t)) \end{bmatrix} \\ z(t) &= y_2(t) \end{aligned} \tag{31}$$

The resulting deviation error dynamics are locally asymptotically stable with $\kappa = [0, 2.5, 0]^\top$. For the numerical simulations in Figure 8 the coupling gain κ_{32} is changed from zero to 2.5 after 150 time units. Notice that although the systems synchronize to each other, the resulting behavior is now that of the selfexcited attractor in both systems, this is change is due to the effect of the coupling terms that before dissipating move the solutions to the basin of attraction of the selfexcited attractor making the hidden attractor solution unreachable.

5. CONCLUSION

We proposed a general framework to solve the synchronization problem of two dynamical systems in *drive-response* and *bidirectional* coupling configurations. The general nature of the proposed synchronization design scheme allows to show that in the case of dynamical systems with hidden and selfexcited attractors the resulting behaviors have particularities. Our results show that in the *drive-response* configuration is relatively simple to impose a synchronized behavior be it of a hidden or a selfexcited attractor, e.g. examples one and three. However, in a *bidirectional* configuration the region of attraction of the synchronized behavior changes and while for a self-excited attractor the design easily is achieved. For a hidden attractor the effect of the coupling terms means that the hidden attractor basically disappears and the resulting behavior is that of a self-excited attractor, as shown in examples two and four. We believe that detail analysis of the basins of attraction for the coupled systems may lead to a design where the synchronized solution be their hidden attractor, investigations in this direction are on their way, and the results will be reported elsewhere.

REFERENCES

Pikovsky, A., Rosenblum, M., Kurths, J.: Synchronization: A Universal Concept in Nonlinear Sciences, Cambridge U. Press, New York (2001)

Boccaletti, S., Kurths, J., Osipov, G., Valladares, D. L., Zhou, C. S.: The synchronization of chaotic systems, Phys Rep, 366, 1–101, (2002)

Pecora, L. M., Carroll, T. L.: Synchronization in chaotic systems, Phys Rev Lett, 64(8), 821–824, (1990)

Rosas Almeida, D. I., Álvarez, Jq., Barajas-Ramírez, J. G.: Robust synchronization of Sprott circuits using sliding mode control, Chaos, Solitons & Fractals, 30(1), 11–18, (2006)

Hong, Y., Qin, H., Chen, G.: Adaptive synchronization of chaotic systems via state or output feedback control, Int J. Bifurc. Chaos, **11**(4), 1148–1158, (2001)

Pan, S., Yin, F.: Optimal Control of Chaos with Synchronization, Int J. Bifurc. Chaos, **7**(12), 2855–2860, (1997)

Boccaletti, S., Latora, V., Moreno, Y., Chavez, M., Hwang, D.-U.: Complex networks: Structure and dynamics, Phys Rep 424, 175–308, (2006)

Su, H., Wang, X.: Pinning Control of Complex Networked Systems Synchronization, Consensus and Flocking of Networked Systems via Pinning, Springer, Shanghai (2013)

Ott, E.: Chaos in dynamical systems, Cambridge Universty Press, Canada (1993)

Leonov, G. A., Kuznetsov, N. V.: Hidden attractors in dynamical systems. From hidden oscillations in Hilbert-Kolmogorov, Aizerman, and Kalman problems to hid-

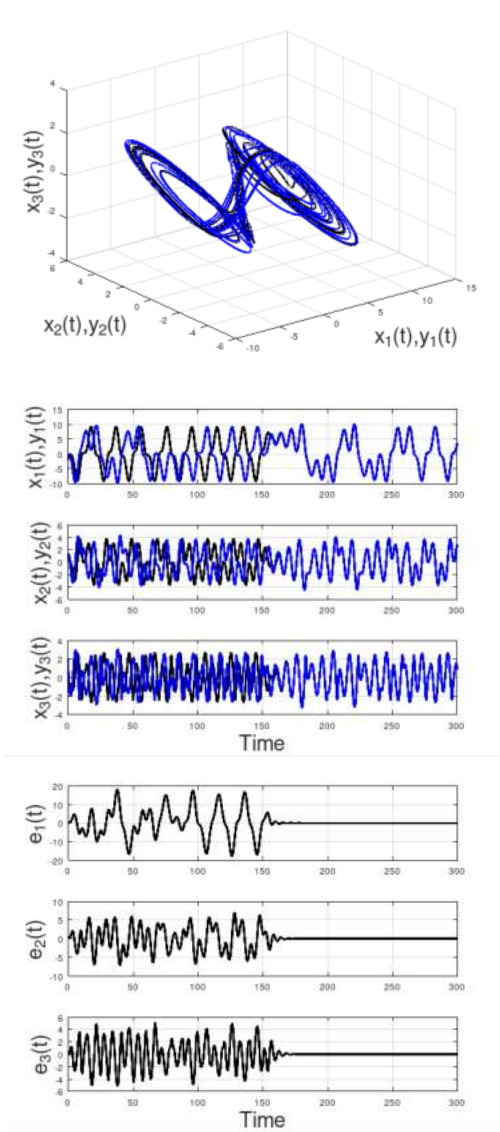

Fig. 8. Synchronization of bidirectionally coupled PWL systems with selfescite and hidden attractor and $\kappa_{32} = 2.5$ for $t > 150$

den chaotic attractor in Chua circuits, Int J. Bifurc. Chaos, 23(1), 1330002, 1–69 (2013)

Pham, V. T., Volos, C., Kapitaniak, T.: Systems with hidden attractors: From theory to realization in circuits, Springer, Switzerland (2017)

Chaudhuri, U., Prasad, A.: Complicated basins and the phenomenon of amplitude death in coupled hidden attractors, Phys Lett A, 378, 713–718 (2014)

Kuznetsov, N. V., Leonov, G. A.: Hidden attractors in dynamical systems: systems with no equilibria, multistability and coexisting attractors, Proc. 19th World Congress IFAC, Cape Town, South Africa, 5445–5454 (2014)

Sprott, J. C.: Some simple chaotic flows, Phys Rev E, **50**, R647 (1994).

Wei, Z.: Dynamical behaviors of a chaotic system with no equilibria, Phys Lett A, 376(2), 102–108 (2011)

Hu, X., Liu, C., Liu, L., Ni, J., Li, S.: Multi-scroll hidden attractors in improved Sprott A system, Nonlinear Dyn, 86, 1725–1734 (2016)

Jafari, S., Sprott, J. C.: Simple chaotic flows with a line equilibrium, Chaos, Solitons & Fractals, 57, 79–84 (2013)

Jafari, M. A., Mliki, E., Akgul, A., Pham, V. T., Kingni, S. T., Wang, X. Jafari, S.: Chameleon: the most hidden chaotic flow, Nonlinear Dyn, 88, 2303–2317 (2017)

Wang, X., Chen, G.: A chaotic system with only one stable equilibrium, Comm. in Nonlinear Sci and Num. Sim., 17(3), 1264–1272 (2012)

Yang, Q., Chen, G.: A chaotic system with one saddle and two stable node-foci, Int J. Bifurc. Chaos, 18, 1393–1414 (2008)

Dudkowski, D., Jafari, S., Kapitaniak, T., Kuznetsov, N. V., Leonov, G. A., Prasad, A.: Hidden attractors in dynamical systems, Phys Rep, 637, 1–50 (2016)

Escalante-González, R. J., Campos-Cantón, E.: Multistable systems with hidden and self-excited scroll attractors generated via piecewise linear systems, Complexity, 2020, 7832489, 1–12, (2020)

Delgado-Aranda, F., Campos-Cantón, I., Tristán-Hernández, E., Salas-Castro, P.: Hidden attractors from the switching linear systems, Revista Mexicana de Física, 66(5), 683–691 (2020)

Escalante-González, R. J., Campos-Cantón, E.: Emergence of Hidden Attractors through the Rupture of Heteroclinic-Like Orbits of Switched Systems with Self-Excited Attractors, Complexity, 2021, 5559913, 1–24, (2021)

Pham, V., Jafari, S., Volos, C., Kapitaniak, T.: Different Families of Hidden Attractors in a New Chaotic System with Variable Equilibrium, Int J. Bifurc. Chaos, 27(9), 1750138 (2017)

Zhang, S., Zeng, Y.: A simple Jerk-like system without equilibrium: Asymmetric coexisting hidden attractors, bursting oscillation and double full Feigenbaum remerging trees, Chaos, Solitons & Fractals, 120, 25–40, (2019)